# Thermal Vacancy Formation and Self-Diffusion in Intermetallic $Fe_3Si$ Nanocrystallites of Nanocomposite Alloys

R. Würschum,[1] P. Farber,[1,2] R. Dittmar,[1] P. Scharwaechter,[1] W. Frank,[1,2] and H.-E. Schaefer[1]
[1]*Universität Stuttgart, Institut für Theoretische und Angewandte Physik, D-70550 Stuttgart, Germany*
[2]*Max-Planck-Institut für Metallforschung, Heisenbergstrasse 1, D-70569 Stuttgart, Germany*
(Received 28 July 1997)

Combined high-temperature studies of positron lifetime and $^{59}Fe$ tracer diffusion show thermal vacancy formation and rapid self-diffusion in the nanocrystallites of intermetallic-amorphous $Fe_{73.5}Si_{13.5}B_9Nb_3Cu_1$ nanocomposites. In combination with an intergranular amorphous phase and densely packed interfaces between these interlayers and the nanocrystallites the unique behavior arises where self-diffusion in interfacial regions is slower than in crystallites. Slow atomic ordering processes during crystallization are ascribed to low diffusivities on the Si sublattice of the nanocrystallites. [S0031-9007(97)04755-8]

PACS numbers: 78.70.Bj, 61.43.Dq, 61.72.Ji, 66.30.Fq

The current interest in the field of nanocrystalline (n-) solids arises from attractive potential applications which are related to crystallite sizes in the nm regime [1]. A central issue in this respect is concerned with the structural stability of nanocrystalline solids at high temperatures. The high-temperature behavior is widely determined by atomic diffusion and thermal vacancy formation, on which, in the case of n-solids, data are still rudimentary and even missing, respectively. This is of fundamental importance because the formation of thermal vacancies in nanocrystalline materials is closely linked to general problems of solid state physics, namely, size effects in fine-dispersed systems and clusters [2,3] and characteristics of thermal defects in disordered systems, such as interfaces and grain boundaries [4].

As an initial step towards an assessment of thermal defect formation in nanocrystalline solids, the present work aims at a combined study [5] of thermal vacancy formation and Fe self-diffusion in the prototype nanocrystalline alloy $Fe_{73.5}Si_{13.5}B_9Nb_3Cu_1$ prepared by crystallization from melt-spun amorphous precursors [6]. In this relatively stable nanocomposite structure with Fe-Si nanocrystallites embedded in an amorphous intergranular matrix (see, e.g., Refs. [7–10]) the thermal-equilibrium formation of vacancies in nanometer-sized crystallites has been detected by positron lifetime spectroscopy for the first time. Based on these results the unique behavior of the FINEMET nanocomposite, i.e., the fact that the Fe diffusion in the crystallites is faster than in the interfaces, can be understood.

In addition to the fast vacancy-mediated diffusion in FINEMET, the present tracer-diffusion and positron-annihilation studies shed light on the ordering processes in the $D0_3$-type nanocrystallites which are substantially determined by the slow atomic motion on the Si sublattice of the nanocrystallites. This provides a guideline for the understanding of the complicated crystallization kinetics [11] (see also [12] and references therein) and for the tailoring of the soft-magnetic properties of FINEMET [13].

In the $^{59}Fe$ diffusion studies the radiotracer atoms were evaporated on polished surfaces of melt-spun $Fe_{73.5}Si_{13.5}B_9Nb_3Cu_1$ specimens which were crystallized at temperatures $T_{crys}$ between 793 and 818 K. After diffusion annealing in vacuum the activity profiles were determined by ion-beam sectioning [14]. In the positron lifetime studies (see [15]) up to 933 K a metallic $^{58}Co$ positron source in a sandwich arrangement with melt-spun ribbons was used.

The $^{59}Fe$ diffusion profiles in nanocrystalline $Fe_{73.5}Si_{13.5}B_9Nb_3Cu_1$ exhibit Gaussian shapes (Fig. 1). This is due to the structural stability during the Fe diffusion process, whereas in nanocrystalline pure metals strongly curved penetration profiles occur due to concomitant crystallite growth and interface migration [16]. Unlike a decrease of the diffusivity which usually occurs upon crystallization [17], a $^{59}Fe$ diffusivity, $D_{nano}$, higher than $D_{amorph}$ in the amorphous state is observed in nanocrystalline $Fe_{73.5}Si_{13.5}B_9Nb_3Cu_1$ (Figs. 1 and 2). With increasing crystallization temperature

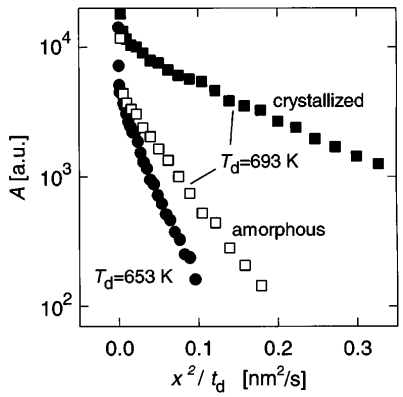


FIG. 1. $^{59}Fe$ diffusion profiles in relaxed amorphous (□) and nanocrystalline (■, •) $Fe_{73.5}Si_{13.5}B_9Nb_3Cu_1$ (FINEMET) crystallized at $T_{crys} = 810$ K for $t_a = 1$ h ($A$: specific radioactivity). $T_d$ and $t_d$ denote the diffusion temperature and time, respectively.

 0031-9007/97/79(24)/4918(4)$10.00 

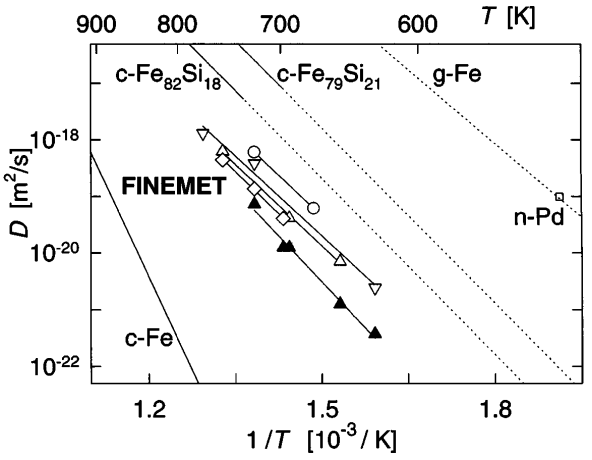


FIG. 2. Arrhenius plots of $^{59}$Fe-tracer diffusivities in nanocrystalline $Fe_{73.5}Si_{13.5}B_9Nb_3Cu_1$ (FINEMET) crystallized at $T_{crys} = 793$ K (◊), 810 K (△), 813 K (▽), 818 K (○), and in the relaxed amorphous state (▲, preannealed at 723 K) prior to crystallization. Literature data are shown for comparison (extrapolations are dotted): Fe diffusion in cluster-compacted nanocrystalline Pd (□, [16]), in the ferromagnetic phase of crystalline $\alpha$-Fe ($c$-Fe, [34]), in grain boundaries of Fe ($g$-Fe, [23]) as well as in the intermetallic compounds $D0_3$-$Fe_{79}Si_{21}$ and $D0_3$-$Fe_{82}Si_{18}$ [18].

the diffusion coefficient increases to a maximum value $D_{nano} \simeq 14 \times D_{amorph}$ (Fig. 2).

The enhanced diffusivity in n-$Fe_{73.5}Si_{13.5}B_9Nb_3Cu_1$ is ascribed to the rapid Fe diffusion in the Fe-Si nanocrystallites which are formed upon crystallization. According to x-ray diffraction (present study and [7,10]) and Mössbauer spectroscopy [7–9] the Fe-Si nanocrystallites exhibit a $D0_3$ structure with a Si content of 18–21 at. %. Single-crystalline $D0_3$-type Fe-Si compounds within this compositional range show extremely high $^{59}$Fe diffusivities [18], which originate from a high concentration of thermal vacancies [19]. Since the diffusion in the nanocrystalline state appears to be slower than in the single-crystalline state (Fig. 2), we conclude that the diffusion process is limited by the crystallite interfaces. This is an exceptional case which is not considered in the Harrison classification scheme of interface diffusion [20]. Self-diffusion faster in crystallites than in interfaces has been taken into consideration for $ZrO_2$-based ionic conductors [21]. In this case the diffusivity in the crystalline state is very high due to a high concentration of dopant-induced oxygen vacancies [21]. In the present case of a metallic nanocomposite the high crystal diffusivity is again due to a high concentration of vacancies which are, however, formed in thermal equilibrium (see below).

A simple diffusion model in which the crystallites (diameter $d$ 12 nm) and the interfaces with the amorphous intergranular phase (thickness $\delta$) are treated as successive layers perpendicular to the direction of diffusion yields the relationship

$$\frac{\delta + d}{D_{nano}} = \frac{\delta}{D_{IF}} + \frac{d}{D_V} \qquad (1)$$

between the experimentally determined diffusion coefficient $D_{nano}$ and the diffusion coefficients in the crystallites ($D_V$) and the interfaces ($D_{IF}$). In the present case of rapid diffusion in the crystallites, $D_V \gg D_{nano}$, Eq. (1) reads

$$D_{IF} = \frac{\delta}{\delta + d} \times D_{nano} = 0.12 \times D_{nano}\,, \qquad (2)$$

with the interface thickness $\delta = 1.6$ nm as estimated from the volume fraction (40%) of the amorphous intergranular phase obtained from x-ray diffraction (present work) and Mössbauer spectroscopy [7]. Together with Eq. (2) the experimental result $D_{nano} = 10 - 14 \times D_{amorph}$ after crystallization at $T_{crys} = 818$ K (Fig. 2) leads to the conclusion that the diffusivity $D_{IF}$ in the amorphous interfaces is similar to that measured in the relaxed amorphous state prior to crystallization (Fig. 2) which is characteristic of Fe-B-Si amorphous alloys [22].

The interfacial diffusivity is substantially lower than in grain boundaries of coarse-grained or nanocrystalline pure metals (see Fig. 2 and [16]) and reflects a dense intergranular phase. This conclusion is supported by the activation energy $Q^{SD} = 1.9$ eV for the $^{59}$Fe diffusion following from the temperature dependence of $D_{nano}$, which is higher than the activation energy $Q_{GB} = 1.7$ eV of the grain-boundary self-diffusion in Fe [23] and still higher than the value $Q_{GB}$ which might be expected for grain boundaries in $D0_3$-$Fe_{79}Si_{21}$ on the basis of the activation energy $Q_V = 2.04$ eV of the Fe volume diffusion [18].

According to the preceding considerations, the unusual diffusion behavior of FINEMET appears to arise from the combination of a high thermal-vacancy concentration in the nanocrystallites *and* a dense interface structure due to an intergranular amorphous phase. Both properties are confirmed by positron lifetime studies, as discussed in the following.

In nanocrystalline $Fe_{73.5}Si_{13.5}B_9Nb_3Cu_1$ the existence of the same type of free volumes as in the amorphous state, but of smaller size than a lattice vacancy, is indicated by the single positron lifetime $\tau_{IF} = 144$ ps observed at ambient temperature (Fig. 3 and [24]). Since positrons in nanocrystalline materials are trapped and annihilated in interfacial regions [25,26], this demonstrates that both the amorphous intergranular layers, which are deduced from x-ray diffraction or Mössbauer spectroscopy [7], and the interfaces between these interlayers and the $Fe_{80}Si_{20}$ nanocrystallites exhibit a densely packed structure. This direct evidence for a densely packed structure of the crystallite-amorphous interfaces is in accordance with the low specific energy of this type of interfaces [27] and supports structural models of crystal-melt interfaces [28].

The reversible high-temperature increase of the mean positron lifetime $\bar{\tau}$ (Fig. 3) is due to the trapping of positrons at thermally formed vacancies in the crystallites. Since, because of the small crystallite size, positron trapping at the interfaces is entirely reaction controlled

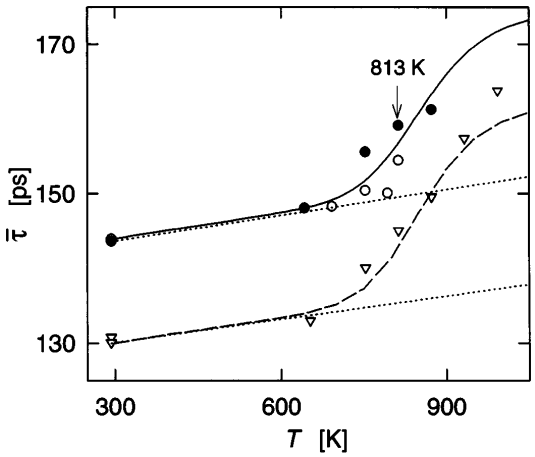


FIG. 3. Thermal vacancy formation in $Fe_{73.5}Si_{13.5}B_9Nb_3Cu_1$ (FINEMET). Mean positron lifetime $\bar{\tau}$ in the nanocrystalline state after annealing at 813 K for 1 h (○) or 21 h (●) and in the microcrystalline state after annealing at 993 K for 31 h (▽). The solid curve is a numerical fit according to Eq. (3). The dotted straight lines show $\bar{\tau}$ in the absence of thermal vacancy formation, assuming a linear temperature variation $\tau_{\text{nano}} = \tau_{\text{nano,293 K}} \times [1 + 10^{-4}(T - 293\,\text{K})]$ like in the free state of pure metals [15].

(specific trapping rate $\alpha$) [26], at high temperatures

$$\bar{\tau} = \frac{(6\alpha/d)\tau_{\text{IF}} + \sigma C_{\text{V}}\tau_{\text{V}}}{6\alpha/d + \sigma C_{\text{V}}} \tag{3}$$

is the trapping-rate averaged value of the positron lifetimes in the interfaces ($\tau_{\text{IF}}$) and the thermal lattice vacancies ($\tau_{\text{V}}$) which compete as positron traps. A numerical fit of Eq. (3) yields for the vacancy formation enthalpy $H_{\text{V}}^{\text{F}} = 1.1$ eV, assuming $\tau_{\text{V}} = 175$ ps and a preexponential factor of the trapping rate $\sigma C_{\text{V}}$ as in single-crystalline $D0_3$-$Fe_{79}Si_{21}$ [19] as well as $\alpha = 200$ m/s as estimated for grain boundaries in Zn alloys [29]. The low value of the vacancy formation enthalpy is identical with that in $D0_3$-$Fe_{79}Si_{21}$ [19] indicating a negligible particle-size effect on the thermal vacancy formation in these crystallites. This is in agreement with calculations of the cohesion energy of metal clusters which reaches the bulk value when the cluster size exceeds ~1000 atoms [3]. Furthermore, this supports the aforementioned conclusion according to which the increase of the $^{57}$Fe tracer diffusivity in $Fe_{73.5}Si_{13.5}B_9Nb_3Cu_1$ upon crystallization is due to a rapid diffusion in the nanocrystallites similar to that in single-crystalline $D0_3$-$Fe_{79}Si_{21}$ [18]. Other causes of the enhanced $D$ value in FINEMET thus appear rather unlikely. For example, an enhanced diffusivity in the intergranular amorphous layer due to a chemical composition which differs from that of the initial amorphous state may be safely excluded [5].

It should be mentioned briefly that after further annealing at $T_{\text{a}} = 933$ K where crystallite growth occurs and Fe-B phases are formed additionally, the positron lifetimes change (Fig. 3). The decrease of the positron lifetime at ambient temperature indicates partial annihilation in the free state of the crystallites when the crystallite size exceeds the diffusion length of positrons [26]. The high-temperature increase of $\bar{\tau}$ is due to thermal vacancy formation in the microcrystalline multiphase structure.

Remarkable features of the present studies are the substantial variations of the diffusion behavior and the thermal vacancy formation with the temperature or time of crystallization (Figs. 2 and 3). As a consequence, both tracer diffusion and positron annihilation may serve as specific indicators of the atomistics of crystallization. This will be exploited in the following.

The increase of the Fe diffusivity by a factor of 4 upon increasing the crystallization temperature from 793 to 818 K (Fig. 2) is ~18× higher than the value which is expected from the concomitant minor increase of the degree of crystallization from 55% to 60% according to Eq. (2). The assumption $D_{\text{V}} \gg D_{\text{nano}}$ leading to Eq. (2) is therefore not applicable to the nanocomposite structure produced by crystallization at $T_{\text{crys}} = 793$ K. The diffusivity in the crystallites of this structure is reduced in comparison to that after higher crystallization temperatures; it is of the same order of magnitude as in the intergranular phase. This variation of the diffusivity with $T_{\text{crys}}$ is confirmed by the variation of the positron lifetime with the crystallization time where thermal vacancies could only be detected after long times of crystallization at 813 K (○ and ● in Fig. 3). The behavior at reduced crystallization temperatures ($T_{\text{crys}} =$ 793 K) or correspondingly small crystallization times is attributed to a reduced Si content or a lower degree of order of the nanocrystallites. In fact, in the coarse-grained intermetallic compound $Fe_3Si$ the Fe diffusivity is observed to decrease with decreasing Si content or degree of order [18] due to a decrease of the thermal vacancy concentration $C_{\text{V}}$ [19]. The decrease of $C_{\text{V}}$ may arise from a concomitant decrease of the fraction of the Fe sites with 4 Si atoms on nearest-neighbor (nn) sites where thermal vacancy formation is favored due to a low nn-bond energy.

Structural ordering or change of composition of the $Fe_3Si$ nanocrystallites requires diffusion on both sublattices. The processes which lead to increases of the Fe diffusivity (Fig. 2) and the thermal vacancy concentration (Fig. 3) with increasing temperature or time of crystallization are therefore controlled by the Si diffusivity, which is much slower than the Fe diffusivity [18]. This is substantiated by considering the processes which are relevant for structural changes. Provided these changes occur due to atomic transport over half the crystallite size (6 nm) on the time scale of crystallization (1 h), a diffusivity of $D \simeq 5 \times 10^{-21}$ m$^2$ s$^{-1}$ must be involved. This compares well with the Ge diffusivity $D_{\text{Ge}}(818\,\text{K}) = 2.5 \times 10^{-21}$ m$^2$ s$^{-1}$ in $D0_3$-$Fe_{82}Si_{18}$ which is expected to be similar to the diffusivity of Si [18]. Furthermore, the annealing of the stress-induced magnetic anisotropy in FINEMET [13] on the time scale of 1 h at 813 K or 20 h at 753 K can be quantitatively understood if it is controlled by such

a low Si diffusivity. Presumably, this slow process also triggers structural modifications at small crystallite growth rates in the advanced state of crystallization whose occurrence was recently concluded from Mössbauer spectroscopy [9,30], x-ray diffraction [31], and measurements of electrical resistivity [11,32]. On the other hand, the Si diffusivity and therefore structural changes are negligible at reduced temperatures or short times where the structure of the nanocomposite is sensitively probed by the rapid Fe diffusion (Fig. 2).

In conclusion, we state that combined high-temperature studies of positron lifetime and $^{59}$Fe-tracer diffusion have led to the detection of vacancy-mediated rapid self-diffusion in nanocrystallites of n-$Fe_{73.5}Si_{13.5}B_9Nb_3Cu_1$. These investigations may be extended to structurally stabilized nanocrystalline metals [33] in order to assess the relation between thermal vacancy formation and diffusion in grain boundaries of metals [4].

The authors are indebted to G. Herzer (Vakuumschmelze Hanau) for supplying the specimen material. Financial support of Deutsche Forschungsgemeinschaft (SFB 277, Project No. B9) is appreciated.

[1] *Nanomaterials: Synthesis, Properties, and Applications*, edited by A. S. Edelstein and R. C. Cammarata (Institute of Physics, Bristol, 1996).
[2] I. D. Morokhov, V. I. Zubov, and V. B. Fedorov, Sov. Phys. Solid State **251**, 178 (1983); C. Baladrón, J. A. Alonso, and M. P. Iñiguez, Phys. Rev. B **37**, 8436 (1988).
[3] H.-G. Fritsche, Z. Phys. Chem. **191**, 219 (1995).
[4] T. Kwok, P. S. Ho, S. Yip, R. W. Balluffi, P. D. Bristowe, and A. Brokman, Phys. Rev. Lett. **47**, 1148 (1981); G. Martin, D. A. Blackburn, and Y. Adda, Phys. Status Solidi **23**, 223 (1967).
[5] R. Würschum, Habilitation thesis, Universität Stuttgart, 1997.
[6] Y. Yoshizawa, S. Oguma, and K. Yamauchi, J. Appl. Phys. **64**, 6044 (1988); G. Herzer, IEEE Trans. Magn. **25**, 3327 (1989).
[7] G. Hampel, A. Pundt, and J. Hesse, J. Phys. Condens. Matter **4**, 3195 (1992).
[8] G. Rixecker, P. Schaaf, and U. Gonser, J. Phys. Condens. Matter **4**, 10 295 (1992).
[9] M. Knobel, R. Sato Turtelli, and H. R. Rechenberg, J. Appl. Phys. **71**, 6008 (1992).
[10] N. Mattern, M. Müller, A. Danzig, and U. Kühn, Nanostruct. Mater. **6**, 625 (1995).
[11] P. Allia, M. Baricco, P. Tiberto, and F. Vinai, J. Appl. Phys. **74**, 3137 (1993).
[12] B. Damson and R. Würschum, J. Appl. Phys. **80**, 747 (1996).
[13] B. Hofmann and H. Kronmüller, J. Magn. Magn. Mater. **152**, 91 (1996).
[14] K. Maier, Phys. Status Solidi A **44**, 567 (1977).
[15] H.-E. Schaefer, Phys. Status Solidi A **102**, 47 (1987).
[16] R. Würschum, A. Kübler, S. Gruß, P. Scharwaechter, W. Frank, R. Z. Valiev, R. R. Mulyukov, and H.-E. Schaefer, Ann. Chim. **21**, 471 (1996); R. Würschum, K. Reimann, and P. Farber, Defect Diffus. Forum **143–147**, 1463 (1997).
[17] T. Schuler, J. Pavlovský, P. Scharwaechter, W. Ulfert, and W. Frank, Nanostruct. Mater. **6**, 863 (1995).
[18] A. Gude, B. Sepiol, G. Vogl, and H. Mehrer, Defect Diffus. Forum **143–147**, 351 (1997); A. Gude and H. Mehrer, Philos. Mag. A **76**, 1 (1997).
[19] E. A. Kümmerle, K. Badura, B. Sepiol, H. Mehrer, and H.-E. Schaefer, Phys. Rev. B **52**, 6947 (1995).
[20] I. Kaur, Y. Mishin, and W. Gust, *Fundamentals of Grain and Interphase Boundary Diffusion* (John Wiley, Chichester, 1995).
[21] M. Filal, C. Petot, M. Mokchah, C. Chateau, and J. L. Carpentier, Solid State Ion. **80**, 27 (1995).
[22] W. Ulfert, J. Horváth, and W. Frank, Cryst. Lattice Defects Amorphous Mater. **18**, 519 (1989).
[23] J. Bernardini, P. Gas, E. D. Hondros, and M. P. Seah, Proc. R. Soc. London A **379**, 159 (1982).
[24] R. Würschum, W. Greiner, R. Z. Valiev, M. Rapp, W. Sigle, O. Schneeweiss, and H.-E. Schaefer, Scr. Metall. Mater. **25**, 2451 (1991).
[25] R. Würschum, Nanostruct. Mater. **6**, 93 (1995).
[26] R. Würschum and A. Seeger, Philos. Mag. A **73**, 1489 (1996).
[27] Y. Nishi, in *Rapidly Quenched Metals*, edited by S. Steeb and H. Warlimont (Elsevier, Amsterdam, 1985), p. 231.
[28] F. Spaepen, Acta Metall. **23**, 729 (1975).
[29] A. Dupasquier, R. Romero, and A. Somoza, Phys. Rev. B **48**, 9235 (1993).
[30] T. Pradell, N. Clavaguera, Jie Zhu, and M. T. Clavaguera-Mora, J. Phys. Condens. Matter **7**, 4129 (1995).
[31] A. Danzig, N. Mattern, and S. Doyle, Nucl. Instrum. Methods Phys. Res., Sect. B **97**, 465 (1995).
[32] P. Duhaj, P. Švec, D. Janičkovič, and I. Maťko, Mater. Sci. Eng. A **133**, 398 (1991).
[33] A. B. Lebedev, S. A. Pulnev, V. I. Kopylov, Yu. A. Burenkov, V. V. Vetrov, and O. V. Vylegzhanin, Scr. Mater. **35**, 1077 (1996).
[34] M. Lübbehusen and H. Mehrer, Acta Metall. Mater. **38**, 283 (1990).